

## NEWS

OF THE NATIONAL ACADEMY OF SCIENCES OF THE REPUBLIC OF KAZAKHSTAN  
PHYSICO-MATHEMATICAL SERIES

ISSN 1991-346X

<https://doi.org/10.32014/2020.2518-1726.81>

Volume 5, Number 333 (2020), 43 – 52

UDC 524.354.6, 52:531.51; 52:530.12; 536.48

IRSTI.29.15.33; 41.17.15; 41.17.41; 41.17.31

A. Tlemissov<sup>1</sup>, Zh. Tlemissova<sup>1,2</sup>, K. Boshkayev<sup>1,2,3</sup>, A. Urazalina<sup>1,2</sup>, H. Quevedo<sup>4,5,1</sup>

<sup>1</sup>Al-Farabi Kazakh National University, Almaty, Kazakhstan;

<sup>2</sup>National Nanotechnology Laboratory of Open Type, Almaty, Kazakhstan;

<sup>3</sup>Fesenkov Astrophysical Institute, Almaty, Kazakhstan;

<sup>4</sup>Instituto de Ciencias Nucleares, Universidad Nacional Autónoma de México, Mexico;

<sup>5</sup>Dipartimento di Fisica and ICRA, Università di Roma “La Sapienza”, Roma, Italy.

E-mail: [Tlemissov-Ozzy@mail.ru](mailto:Tlemissov-Ozzy@mail.ru); [kuantay@mail.ru](mailto:kuantay@mail.ru)

## ANALYSIS OF THE EQUATIONS OF STATE FOR NEUTRON STARS

**Abstract.** In this work we consider various equations of state of neutron star matter, which include from the point of neutron drops formation to supra nuclear densities. Particular attention is paid to the nucleon – nucleon interaction since, in addition to the kinetic energies of the particles, the interactions among nucleons play a key role. Moreover, we investigate the properties of super-dense matter with diverse sets of particles such as electrons, protons, and the contribution of various particles-carriers of interaction. In order to achieve these goals, different potentials were considered, which are in a good agreement with experimental data. Furthermore, we find the energy of the system by using a variety of multi-particle methods, including the interaction of nucleons. Thanks to this information, thermodynamic parameters such as pressure, energy density and the speed of sound in the star are calculated. We compared similar equations of state of matter so that we could demonstrate the difference from each other. The Tolman-Oppenheimer-Volkoff system of equations has been solved numerically to construct mass-central density, radius-central density and mass-radius relations using different equations of state. In conclusion, the latest observational constraints on the equation of state are taken into account and we show that the observational data require that the equation of state be stiff, despite the fact that all stiff equations of state violate the principle of causality at high central densities, unlike soft ones.

**Keywords:** Equation of state, neutron stars, nuclear interactions, observational constraints.

**1. Introduction.** First theoretical calculations on the properties of neutron stars were carried out at the beginning of the 20th century by Tolman and Oppenheimer. It was shown that with increasing mass of a star, the electron pressure is no longer able to oppose the gravitational compression. Whereas the electrostatic corrections do not make a large contribution to the pressure of the star in the descriptions of white dwarf stars and were often neglected, the interactions between nucleons become crucial as the matter density becomes close to the nuclear density. The attraction between the nucleons reduces the pressure, but the repulsion caused by vector carriers increases the pressure, thereby preventing the collapse of the star [1]. If the Fermi energy is large, then in addition to neutrons other particles are formed in the neutron star. The Baym equation of state (EoS), which includes neutrons, protons and electrons, describes well neutron star matter at densities below the formation of neutron drops  $\rho_{drip} = 4.3 \times 10^{11} \text{ g/cm}^3$  then it goes quite smoothly into the Baym-Bem-Petrik EoS [2], which in turn describes the state of matter within  $\rho_{drip} < \rho < \rho_{nuc}$ , where  $\rho_{nuc} = 2.8 \times 10^{14} \text{ g/cm}^3$  – nuclear density. Further, the results vary widely within the densities above the density of nuclear matter. This is the range we will investigate in this work. The structure of the paper is organized as follows: in sections 2 and 3, a neutron star is considered at zero temperatures for the EoS of a degenerate neutron gas. In sections 4, 5, and 6, different equations of state (EoS) are compared, taking into account the interactions between particles. In section 7, the main results are discussed and the corresponding conclusions are summarized.

**2. Pure neutron gas.** The pressure of a degenerate neutron gas is calculated in the so-called phase spaces. With an increase in the density of a neutron star, the uncertainty principle greatly increases the momentum phase space and the radius of the star decreases. Further, due to the gravitational instability, it will decrease to the gravitational radius  $r_g = 2GM/c^2$  where the inner structure of the star is destroyed and a black hole is formed. Here  $G$  is the gravitational constant,  $c$  is the speed of light in vacuum and  $M$  is the total mass of the star. We write the relativistic hydrostatic equilibrium equation, Tolman-Oppenheimer-Volkoff (TOV) equation, for a perfect fluid as:

$$\begin{cases} \frac{dm(r)}{dr} = \frac{4\pi r^2}{c^2} \varepsilon(r) \\ \frac{dp(r)}{dr} = -\varepsilon(r) \frac{Gm(r)}{c^2 r^2} \left[ 1 + \frac{p(r)}{\varepsilon(r)} \right] \left[ 1 + \frac{4\pi r^3 p(r)}{c^2 m(r)} \right] \left[ 1 - \frac{2Gm(r)}{c^2 r} \right]^{-1} \end{cases} \quad (1)$$

where  $\varepsilon(r) = c^2 \rho(r)$  is the energy density of hadron matter,  $p(r)$  is the pressure,  $\rho(r)$  is the density,  $m(r)$  is the mass of matter inside a sphere enclosed within radius  $r$ . This is a system of first-order ordinary differential equations, the solutions of which should represent equilibrium configurations of a perfect fluid with density  $\varepsilon(r)$  and pressure  $p(r)$ . The TOV equation cannot be solved in its present form because it is an open system of differential equations. To close it, we must add an equation, which is usually given in the form of an EoS (EoS). Clearly, not every EoS can be used to generate physically reasonable solutions of the TOV equation. In fact, not every EoS can lead to an equilibrium configuration. In the case of a neutron star an appropriate EoS can be written in a parametric form as:

$$\begin{cases} \varepsilon(r) = \frac{\varepsilon_0}{8} \left[ (2y(r)^3 + y(r))\sqrt{1+y(r)^2} - \ln(y(r) + \sqrt{1+y(r)^2}) \right] \\ p(r) = \frac{\varepsilon_0}{24} \left[ (2y(r)^3 - 3y(r))\sqrt{1+y(r)^2} + 3\ln(y(r) + \sqrt{1+y(r)^2}) \right] \end{cases} \quad (2)$$

where,  $y(r) = k_n(r)/m_n c$ ,  $k_n(r)$  is the dimensionless Fermi momentum of a neutron,  $\varepsilon_0 = m_n^4 c^5 / \pi^2 \hbar^3$  constant having the dimension of energy density [3]. We introduce the dimensionless energy density and pressure in the following form  $\varepsilon = \bar{\varepsilon} c^4 / Gb^2$ ,  $p = \bar{p} c^4 / Gb^2$ ,  $\rho = \bar{\rho} c^2 / Gb^2$ , where  $\bar{\rho}$  is the dimensionless density,  $\bar{p}$  is the dimensionless pressure,  $\bar{\varepsilon}$  is the dimensionless energy density. To make systems of equations (1) and (2) dimensionless we introduce the quantities  $r = bx$ ,  $m = \bar{m} c^2 b / G$ , where  $b = \pi \sqrt{\hbar^3 / Gc m_n^4}$  is a parameter with dimension of length, satisfying the equality  $\varepsilon_0 = c^4 / Gb^2$  [3],  $x$  is dimensionless radial coordinate, and  $\bar{m}$  is the dimensionless mass. Then, the EoS (2) reduces to

$$\begin{cases} \bar{\varepsilon}(x) = \frac{1}{8} \left[ (2y(x)^3 + y(x))\sqrt{1+y(x)^2} - \ln(y(x) + \sqrt{1+y(x)^2}) \right] \\ \bar{p}(x) = \frac{1}{24} \left[ (2y(x)^3 - 3y(x))\sqrt{1+y(x)^2} + 3\ln(y(x) + \sqrt{1+y(x)^2}) \right] \end{cases} \quad (3)$$

and the structure equations (1) become

$$\begin{cases} \frac{d\bar{m}(x)}{dx} = 4\pi x^2 \bar{\varepsilon}(x) \\ \frac{d\bar{p}(x)}{dx} = -\bar{\varepsilon}(x) \frac{\bar{m}(x)}{x^2} \left[ 1 + \frac{\bar{p}(x)}{\bar{\varepsilon}(x)} \right] \left[ 1 + \frac{4\pi x^3 \bar{p}(x)}{\bar{m}(x)} \right] \left[ 1 - \frac{2\bar{m}(x)}{x} \right]^{-1} \end{cases} \quad (4)$$

equations (3)-(4) describe the behavior of matter at densities below the formation of neutron droplets and above nuclear matter.

**3. Neutron stars with protons, electrons.** The pressure caused by protons and electrons in a neutron star is small, but it is still present and softens the EoS by slightly reducing the maximum mass. In order to

achieve equilibrium the electro-neutrality condition  $n_e = n_p$ , where  $n$  is the particle number density [4], along with a balance between reactions  $n \rightarrow p + e + \bar{\nu}_e$  and  $p + e \rightarrow n + \nu_e$  must be fulfilled within the star. Hence, the EoS is constructed in the same way as for degenerate noninteracting neutrons and has the following form [5]:

$$\begin{cases} \varepsilon(r) = \pi \sum_{i=n,p,e} \frac{m_i c^2}{\Lambda_i^3} \left[ (2y_i(r)^3 + y_i(r)) \sqrt{1 + y_i(r)^2} - \ln(y_i(r) + \sqrt{1 + y_i(r)^2}) \right] \\ p(r) = \frac{\pi}{3} \sum_{i=n,p,e} \frac{m_i c^2}{\Lambda_i^3} \left[ (2y_i(r)^3 - 3y_i(r)) \sqrt{1 + y_i(r)^2} + 3 \ln(y_i(r) + \sqrt{1 + y_i(r)^2}) \right] \end{cases} \quad (5)$$

where, the Compton wavelength of particles are  $\Lambda_n = 1.319 fm$ ,  $\Lambda_p = 1.321 fm$ ,  $\Lambda_e = 2.42 \times 10^3 fm$  and the rest masses are  $m_e c^2 = 0.511 Mev$ ,  $m_p c^2 = 938.272 Mev$ , and the dimensionless Fermi momenta for protons and electrons are given by

$$y_p(x) = \frac{\sqrt{m_e^4 + (m_p^2 - m_n^2(1 + y_n(x)))^2 - 2m_e^2(m_p^2 + m_n^2(1 + y_n(x)))}}{2m_n m_p \sqrt{1 + y_n(x)^2}}, \quad y_e = y_p \quad (6)$$

where for convenience we have denoted  $m_i c^2 = m_i$ . The Fermi momentum can be calculated from the condition that the lower threshold for the neutron formation at  $y_n(x) = 0$  is equal to  $y_p(x) = 0.001265$ ,  $y_e(x) = y_p(x)$ , and central density is  $\rho = 1.186 \times 10^7 g/cm^3$ .

By solving the TOV equations using (5) we get the mass-radius relation for a neutron star depicted in Fig. 1. Note that in the  $M - \rho$  diagram (right panel) the configurations to the left of  $M_{Max}$  are unstable and collapse into a black hole. A similar situation also occurs in the  $M - \rho$  diagram (left panel), only here unstable configurations are to the right of  $M_{Max}$ . It can be seen that the contribution of protons and electrons to the pressure or density and correspondingly to the mass is not significant.

Another feature of the EoS with non-interacting protons, neutrons and electrons is that with increasing Fermi energies, electrons can decay into muons [6], and muons in turn decay into electrons with the emission of neutrinos or anti-neutrinos. This is one of the few ways for cooling of a neutron star at high temperatures [1]. The minimum density at which muons are formed is  $\rho = 8.21 \times 10^{14} g/cm^3$ . At densities  $\rho = 1.36 \times 10^{15} g/cm^3$ ,  $T < T_c = 2.2 \times 10^{11} K$  pion condensate forms [7]. If we take into account that during the formation of a neutron star, the temperature still reaches a value  $T > T_c$ , but due to the neutrino cooling the temperature decreases from  $10^{11}$  until  $10^9 K$  in a month, then the formation of pion condensation in the core of stars is inevitable. It means that, in realistic models and in all EsoS, the curves should strongly move down after  $\rho \approx 10^{15} g/cm^3$ , since pion condensations soften the EoS by decreasing the maximum mass and are highly dependent on the model, though they have no contribution to pressure. As for other pions, for example neutral pions  $\pi^0$  in 98% cases decay into two gamma quanta  $\pi^0 \rightarrow 2\gamma$ , that is, there is an equilibrium state between  $\pi^0 \Leftrightarrow 2\gamma$  but the equation for the chemical potential gives  $\mu_{\pi^0} = 0$ , and for  $\mu_{\pi^+} = -\mu_e < 0$ , therefore, in both cases, the distribution function for  $T = 0K$  tends to  $f = \frac{1}{e^{(E-\mu)/kT} - 1} \rightarrow 0$ . The formation of such particles is not expected in superdense matter, at least not at low temperatures, for the same reason positrons, anti-baryons and other mesons must be absent in an ideal gas [4].

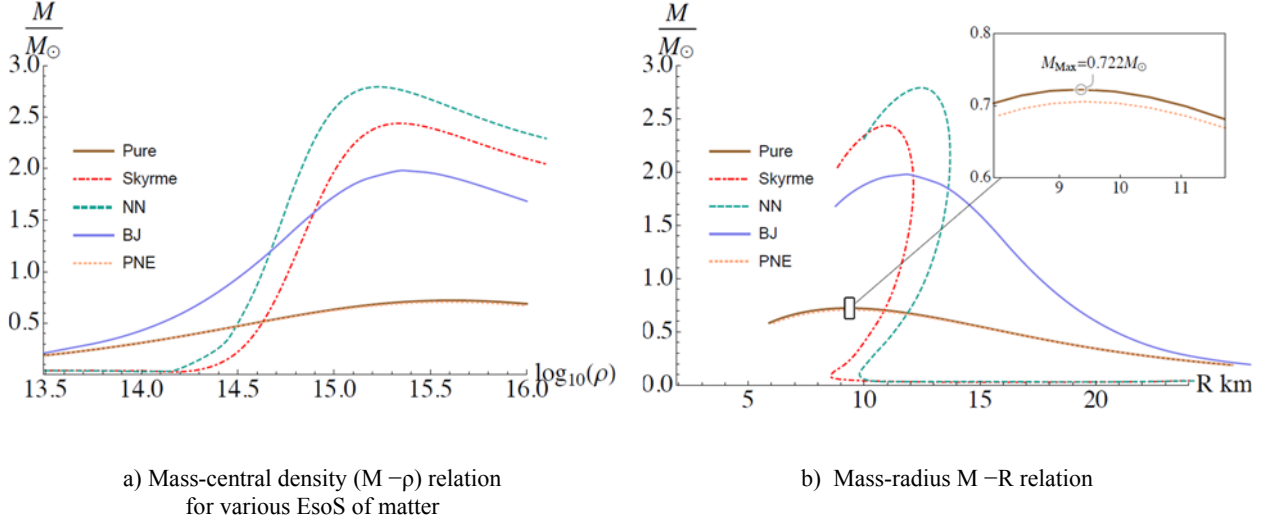


Figure 1 - The mass-central density (in  $\text{g}/\text{cm}^3$ ) and mass-radius relations, NN is the empirical EoS, Skyrme is for the skyrme potential, Pure is the degenerate neutron gas and BJ is the Bethe-Jones EoS. It can be seen that the maximum mass is decreased and is equal to  $M = 0.7057M_{sun}$  at  $R = 9.394 \text{ km}$  if we include electrons and protons into degenerate neutron gas

**4. Bethe-Johnson nuclear interaction.** Almost all EsoS of neutron stars are based on finding the energies of nucleon-nucleon interactions [8]. Nuclear scientists and theoreticians have spent plenty of time and effort studying nucleon-nucleon interactions. From interaction theories it is known that the attraction between nucleons is due to the exchange of scalar fields of pions, and repulsion by vector particles, in particular  $\rho$ ,  $\omega$ ,  $\varphi$  (where  $\rho$ ,  $\omega$ ,  $\varphi$  particle carriers of nuclear matter). Bethe and Johnson only considered repulsion from  $\omega$  ( $783 \text{ MeV}$ ), since it is this particle with nucleons that possesses the strongest coupling constant and is approximately estimated in  $g_{\omega}^2 = /\hbar c = 12.868$  [9], and most importantly, it describes well the experimental data on the binding energy of nucleons and the quadrupole moment of the deuteron. So using the Bethe and Jones potential, taking into account the variational method and considering the agreement with experiments, we obtain an EoS that relates density and pressure through the parametric equations [1]:

$$\begin{cases} \varepsilon = m_n n(x) + \frac{3(3\pi^2)^{2/3}(\hbar c)^2}{10m_n} n(x)^{5/3} + 236n(x)^{a+1} \\ p = n(x)^2 \frac{d(\varepsilon/n)}{dn} = \frac{(3\pi^2)^{2/3}(\hbar c)^2}{5m_n} n(x)^{5/3} + 363n(x)^{a+1} \end{cases} \quad (7)$$

where  $a = 1.54$ ,  $m_n = m_n c^2 \text{ MeV}$  and  $\hbar c = 197.327 \text{ MeV} \times \text{fm}$ . To make equation (7) dimensionless we multiplied by  $G b^2 / c^4 = 1.007 \times 10^{-4} \text{ fm}^3 / \text{MeV}$ . The speed of sound on the surface of a star is equal to

$$\left(\frac{c_s}{c}\right)^2 = \frac{dp}{d\varepsilon} = \frac{0.143n^{2/3} + 0.649n^a}{0.214n^{2/3} + n^a + 1.01} \quad (8)$$

where, the speed of sound is always  $c_s < c$  for any densities in the Bethe-Jones EoS, as well as in the case of a degenerate neutron gas or mixed with protons and electrons. Numerical solutions of the TOV equations are given in figures 1 and 2.

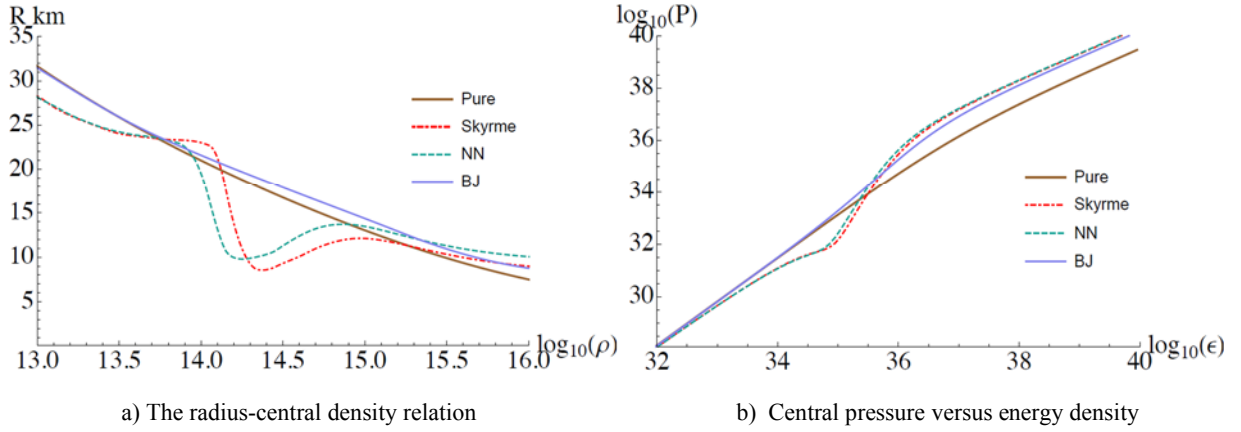


Figure 2 - Dependence of various parameters for the neutron star EoS

**5. Empirical nuclear interaction.** No matter how we choose the interaction potential between nucleons, it must be in agreement with the experimental data, that is, it must lead to the saturation of nuclear matter having satisfied 3 conditions: 1) the number density at which the saturation is achieved  $n_0 = 0.16 \text{ fm}^{-3}$ , 2) the binding energy at saturation  $BE = \frac{E}{A} \Big|_{n=n_0} = -16 \text{ MeV}$ , where  $BE$  is the binding energy, 3) the compressibility of the nuclear matter  $K(n_0) = 9 \frac{dp}{dn} = 400 \text{ MeV}$ , it is known from the experiment that the compressibility value changes depending on the potentials. In our case, a test function for the EoS of symmetric matter  $n_p = n_n$  has the following form:

$$\begin{cases} \varepsilon/n = m_n + \langle E_0 \rangle u^{2/3} + \frac{A}{2} u + \frac{B}{\sigma+1} u^\sigma \\ p/n_0 = \frac{2}{3} \langle E_0 \rangle u^{5/3} + \frac{A}{2} u^2 + \frac{B\sigma}{\sigma+1} u^{\sigma+1} \end{cases} \quad (9)$$

after substituting in the conditions for saturation of the nuclear matter, the constants are equal to  $A = -118.2 \text{ MeV}$ ,  $B = 65.39 \text{ MeV}$ ,  $\sigma = 2.112$ ,  $\langle E_0 \rangle = 22.1 \text{ MeV}$ . A model describing only neutron matter  $n = n_n$  is given by

$$\begin{cases} \varepsilon/n = m_n + 2^{2/3} \langle E_0 \rangle u^{2/3} + \left( \frac{A}{2} - (2^{2/3} - 1) \langle E_0 \rangle + S_0 \right) u + \frac{B}{\sigma+1} u^\sigma, \\ p/n_0 = \frac{2^{5/3}}{3} \langle E_0 \rangle u^{5/3} + \left( \frac{A}{2} - (2^{2/3} - 1) \langle E_0 \rangle + S_0 \right) u^2 + \frac{B\sigma}{\sigma+1} u^{\sigma+1} \end{cases} \quad (10)$$

where  $S_0$  is the volume symmetry coefficient (degree of deviation from symmetry),  $u = n/n_0$ , the range of applicability of the equation is from the order of the nuclear density to  $\rho = 1.135 \times 10^{15} \text{ g/cm}^3$  since beyond this value it will violate the principle of causality.

**6. Skyrme interaction.** In this section, we select a potential that gives a repulsive effect at high concentrations, since at high densities, which is equivalent to the reduction of the distance between nucleons, the repulsive force due to the exchange of vector particles dominates. Based on these arguments we choose the potential in the form of  $V(x-y) = \delta(x-y) \left( \frac{1}{6} t_3 n - t_0 \right)$ , where  $t_0$  is the parameter that

characterizes repulsion owing to the exchange of scalar particles between two nucleons,  $t_3$  is the parameter describing the repulsion at high densities. Next, we find the energy with help of the Hartree-Fock method, if the spin of particles is not considered (the calculation of the same potential using the

method of Hartree) we find that the energy increases twice. This is due to the fact that taking into account the spin of the particles reduces the total energy practical twice because in the first approximations only those pairs interact which have antiparallel spins. The EoS with spin reads as follows:

$$\begin{cases} \varepsilon = m_n n(x) + \frac{3(3\pi^2)^{2/3}(\hbar c)^2}{10m_n} n(x)^{5/3} - \frac{t_3}{24} n(x)^3 - \frac{t_4}{4} n(x)^2, \\ p = \frac{(3\pi^2)^{2/3}(\hbar c)^2}{5m_n} n(x)^{5/3} - \frac{t_3}{12} n(x)^3 - \frac{t_4}{4} n(x)^2, \end{cases} \quad (11)$$

where the constants  $t_3, t_0$  are found from the saturation condition for nuclear matter as well as for nucleon-nucleon interactions. After simple calculations one finds  $t_3 = 14600.8 \text{ MeV}$ ,  $t_0 = 1024.1 \text{ MeV}$ . The domain of applicability of the EoS is  $2.707 \times 10^{14} \text{ g/cm}^3 < \rho < 1.55 \times 10^{15} \text{ g/cm}^3$  [3].

**7. Observational constraint.** The physical constraints imposed on the EoS are known. This is primarily a restriction on the speed of sound, since the speed of sound in the core and on the surface of a star must fulfill the condition  $c_s/c < 1$ , in our cases, these conditions are not met for the skyrme EoS when  $\rho > 1.55 \times 10^{15} \text{ g/cm}^3$  and for the empirical nucleon- nucleon interaction at

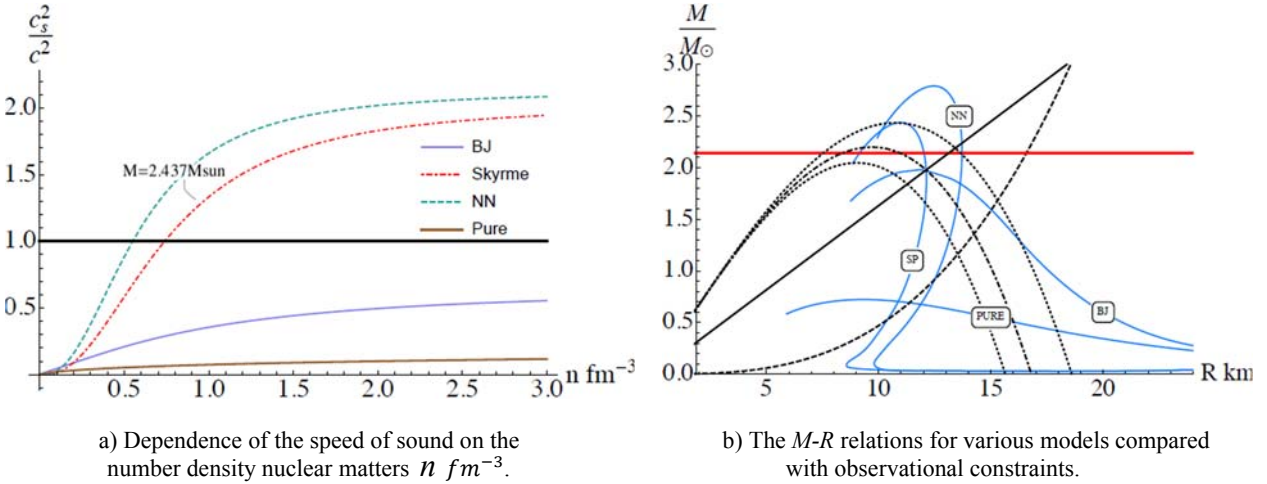


Figure 3 - Various EoS with theoretical and observational constraints

$\rho > 1.135 \times 10^{15} \text{ g/cm}^3$ , in Fig. 3a it can be seen that the maximum mass for the skyrme potential and for the empirical EoS must not exist from the physical point of view, since it lies above the plane  $c_s/c = 1$ . In figure 2 (b) the matter pressure is shown as a function of the energy density. As one can see the behavior of each EoS is different.

As for observational constraints, we learned from collecting data on neutron stars for 2019-2020 year [10] that with 95% confidence the mass of the most massive pulsar PSR J0740+6620, located at a distance of 1500 light years from Earth, lies in the range  $M = 2.14^{+0.20}_{-0.18} M_{\text{Sun}}$  with a rotation period in 2.89 ms (see figures 4c), it is marked with a thick red line. The lowest radius has been observed in the RX J1856-3754 [11]; for an observer at infinity the radius is  $R_{\infty} = R \sqrt{1 - \frac{2GM}{c^2 R}}$  so that for  $R_{\text{min}} = 16.8 \text{ km}$  [12], the

conditions read  $2GM/c^2 R > R - R^3/(R_{\infty}^{\text{min}})^2$  [13]. In figure 3b, this is indicated by a dotted curve and a dotted line. Furthermore, the largest surface gravity of a neutron star is for  $M = 1.4 M_{\text{Sun}}$ .

On the other hand, the observed radius with 90% confidence is  $15.64 \text{ km} < R_{\infty} < 18.86 \text{ km}$ ; in figure 3b, we mark the lower limit of the surface gravity with two dotted curves of the form

$2GM/c^2R > R - R^3/(R_\infty)^2$  [13]. The most famous and fastest rotating neutron star PSR J1748-2246 [14] has the highest rotation frequency 716 Hz and the equation for the frequency is determined as  $v_{\max} = 1045(M/M_{Sun})^{1/2}(10km/R)^{3/2}$ . Therefore, the constraint on the rotation looks like this  $M \geq 0.47(R/10km)^3 M_{Sun}$  and the figure it is shown as a dashed curve. Finally, the upper limit on the surface gravity of a neutron star is determined by the pulsar XTE J1814-338 and the constraint is  $M/M_{Sun} < 2.4 \times 10^5 c^2 R / GM_{Sun}$  shown in the figure as a solid black line [15]. Realistic mass-radius relations must pass through the region surrounded by the observational constraints. Therefore, as one can see, the pure degenerate neutron gas EoS is not realistic.

**8. Discussion and conclusion.** In this paper, we obtained the dependence of mass on radius and on the central density for different EoSs of Neutron Stars. It can be seen in figure 1 that if we do not take into account the nucleon-nucleon interaction, the EoS will be extremely soft to describe the dependence of the mass on the radius, which does not correspond to the observations. In section III, we discussed the appearance of pion condensation, but in realistic models, the formation of condensation must be prevented by many factors such as the pion-nucleon interaction [7]. In Ref. [16] the EoS with protons, neutrons and electrons was studied, but instead of the local electroneutrality condition  $n_p - n_e = 0$  the global electroneutrality condition was used in the form  $\int \rho_{ch} d^3r = \int e[n_p(r) - n_e(r)] = 0$ . At the same time, the Lagrangian density  $L$  takes into account the repulsive force between nucleons from vector bosons  $\rho_\mu$  and  $\omega_\mu$  also the electromagnetic 4-potential  $A_\mu$  or any Lagrangian types [17].

As can be seen from figures 1 and 3, the empirical EoS has the most rigid dependence of mass on radius, but the plots quickly fall down with the inclusion of protons. The equation of Bethe - Jones is in good agreement with the experimental data, but at high densities, it is not enough to describe the repulsive force with a single  $\omega$  meson. Nevertheless, the EoS does not contradict the latest observational and theoretical constraints, which is certainly a big advantage. The EoS for the skyrme potential is just a good description of the matter at high densities up to  $\rho < 5.5\rho_{nuc}$  which corresponds to a star with mass  $M = 2.37M_{Sun}$ .

The final results are shown in figure 3, as expected, the lower limit of observational constraints lies in the interval  $1.3M_{Sun} < M < 1.4M_{Sun}$  that is close to the Chandrasekhar limit, which in turn lies in the range of  $1.38 - 1.44 M_{sun}$  for white dwarf stars. According to some estimates the maximum observed mass of a neutron star PSR J0740+6620 is  $2.17M_{Sun}$ . The existence of such an object is explained by the fact that a rapidly rotating neutron star increases the maximum mass by almost 15%. Apparently, in the past, PSR J0740+6620 absorbed a significant part of the substance of its companion - most likely, when it was still at the stage of the red giant [18].

According to 2015 data, about 2500 neutron stars are known. Out of them, only 10% have companions. Many massive neutron stars also have an inner core. The radius of the inner core can reach up to several kilometers, and the density in the center of the nucleus can exceed the density of atomic nuclei by 7-8 times. The composition and EoS of the substance of the inner core are not known for certain. At such densities, neutrons can give way to hyperons, three-quark particles that include at least one strange quark, or even consist of free quarks and gluons [19].

**Acknowledgement.** This work was supported by Ministry of Education and Science of the Republic of Kazakhstan, Program IRN: BR05236494, Grants IRN: AP05134454 and IRN: AP08052311.

А. Тлемисов<sup>1,2</sup>, Ж. Тлемисова<sup>1,2</sup>, Қ. Бошқаев<sup>1,2,3</sup>, А. Уразалина<sup>1,2</sup> және Э. Кэведо<sup>1,4,5</sup>

<sup>1</sup>Әл-Фараби атындағы Қазақ ұлттық университеті, Алматы, Қазақстан;

<sup>2</sup>Ашық түрдегі ұлттық нанотехнологиялық зертхана, Алматы, Қазақстан;

<sup>3</sup>Фесенков атындағы астрофизикалық институт, Алматы, Қазақстан;

<sup>4</sup>Ядролық ғылымдар институты, Мексика ұлттық автономдық университеті, Мехико, Мексика;

<sup>5</sup>Физика кафедрасы және релятивистік астрофизика халықаралық орталығы,  
Ла Сапиенца Рим университеті, Италия

## НЕЙТРОНДЫҚ ЖҰЛДЫЗДАРДЫҢ КҮЙ ТЕНДЕУЛЕРІН ТАЛДАУ

**Аннотация.** Жұмыста нейтрондық жұлдыздардың, нейтрондық тамшылардың пайда болуынан бастап, асқын ядролық тығыздыққа дейінгі әртүрлі күй теңдеулері: айныған нейтрондық газ, Бета және Джонс күй теңдеуі, эмпирикалық күй теңдеуі және Skyrme потенциалды күй теңдеуі қарастырылған. Алғашқы қадам ретінде Толман-Оппенгеймер-Волковтың релятивтік гидростатикалық тепе-теңдік теңдеуі масса-орталық тығыздық, масса-радиус және радиус-орталық тығыздық қатынасын тұрғызу үшін қолданылды. Себебі нейтрондық жұлдыз таза релятивтік объект. Күй теңдеуін таңдау барысында нейтрондар және кейбір жағдайлар үшін протондар арасындағы нуклон-нуклондық әсерлесуге аса мән берілді. Өйткені, кинетикалық энергиямен қатар нуклондар арасындағы әсерлесу де маңызды рөл атқарады.

Сонымен қатар, нейтроннан басқа электрон және протон сияқты әртүрлі бөлшектер жиынтығынан тұратын аса тығыз материяның қасиеттері және әсерлесуді тасымалдаушы бөлшектердің үлесі зерттелді. Осы мақсатқа жету барысында тәжірибемен жақсы үйлесетін Бета мен Джонс потенциалы және Skyrme потенциалы қарастырылды. Нуклондардың әсерлесуімен қоса, әртүрлі көпбөлшектік әдістері, Хартри және Хартри-Фок әдістері қолданылып, жүйенің энергиясы анықталды. Осы ақпаратқа сүйене отырып қысым, энергия тығыздығы және нейтронды жұлдыздағы дыбыс жылдамдығы сияқты термодинамикалық параметрлер тығыздық функциясы ретінде есептелді. Бір-бірінен айырмашылықтарын көрсету үшін қасиеттері ұқсас келетін заттың күй теңдеулері салыстырылды.

Жалпы алғанда, фундаменталды заңдарды тексеру барысында маңызды астрофизикалық объект болып саналатын миллисекундтық пульсарлар бақыланады. Бақылаудың соңғы нәтижелері күй теңдеулерінің, жұмсақ күй теңдеулеріне қарағанда, жоғарғы тығыздықта себеп-салдар принципін бұзатынына қарамастан, қатаң болуды талап етті. Бұл нәтижелер, айналатын пульсарды бақылау барысында Шапиро эффекті арқылы пульсар массасын анықтауға мүмкіндік беретін физикалық параметрлерді анықтауға болатынын көрсеткен. Солтүстік Америка обсерваториясында гравитациялық толқындар (NANOGrav) үшін наногерц бойынша мәліметтерді біріктіру барысында 12,5 жыл бойы орбиталды фазаны бақылауда Green Bank телескобын қолдана отырып, PSR J0740 + 6620 – нейтрондық жұлдыздың массасы  $2,14_{-0,09}^{+0,10}$  күн массасына тең болатыны анықталды. Біздің есептеуімізде PSR J1748-2246 нейтронды жұлдыздың айналуы стандартты бақылаудан белгілі шектеу болып саналады. Аталған пульсар секундына 1122 айналым жасайтын ХТЕ J1739-285 пульсардан кейін жылдамдығы бойынша екінші болып саналады. Дегенмен басқа астрономдар ХТЕ J1739-285 пульсардың айналу периодын әлі толық растамаған.

Қорытындылай келе, жұмыста әсерлесуді ескермеген есептеу нәтижелері, бір тасымалдаушының әсері ескерілгендегі әсерлесу (Бета және Джонс күй теңдеулері жағдайында) нәтижелерінен едәуір айырмашылық көрсететіні баяндалған. Сонымен қатар, эмпирикалық жолмен тұрғызылған, жұлдыздың толық радиусының орталық тығыздыққа тәуелділігі айныған нейтрондық газдан ерекшеленетіні көрсетілді. Жұмыстың жаңалығы, бақылаудан алынған мәліметтермен қоса, нейтрондық жұлдыздарды сипаттау үшін әртүрлі күй теңдеулерін қолдануда және олардың қайсысы жеткілікті түрде физикалық шынайылықты сипаттайтынын көрсетуге.

**Түйін сөздер:** күй теңдеуі, нейтронды жұлдыз, масса-радиус арақатынасы, ядролық әсерлесу, бақылаудан алынған шектеулер.

А. Тлемисов<sup>1</sup>, Ж. Тлемисова<sup>1,2</sup>, Қ. Бошқаев<sup>1,2,3</sup>, А. Уразалина<sup>1,2</sup> и Э. Кэведо<sup>4,5,1</sup>

<sup>1</sup>Казахский национальный университет им. аль-Фараби, Алматы, Казахстан;

<sup>2</sup>Национальная нанотехнологическая лаборатория открытого типа, Алматы, Казахстан;

<sup>3</sup>Астрофизический институт им. Фесенкова, Алматы, Казахстан;

<sup>4</sup>Институт ядерных наук, Национальный автономный университет Мексики;

<sup>5</sup>Кафедра физики и Международный центр релятивистской астрофизики,  
Римский Университет “Ла Сапиенца”, Рим, Италия

## АНАЛИЗ УРАВНЕНИЙ СОСТОЯНИЯ НЕЙТРОННЫХ ЗВЕЗД

**Аннотация.** В данной работе рассмотрены различные уравнения состояния нейтронных звёзд, такие как уравнение состояния вырожденного нейтронного газа, уравнение состояния Бета и Джонса, эмпирическое



уравнение состояния и уравнение состояния с потенциалом Skyrme, от точки образования нейтронных капель до сверхядерных плотностей. Поскольку нейтронная звезда является чисто релятивистским объектом, было использовано релятивистское уравнение гидростатического равновесия Толмана-Оппенгеймера-Волкова в качестве отправной точки для получения соотношений масса-центральная плотность, масса-радиус и радиус-центральная плотность. При выборе уравнений состояния было уделено особое внимание тем уравнениям, в которых учитывается нуклон-нуклонные взаимодействия между нейтронами, в некоторых случаях с протонами, поскольку кроме кинетической энергии частицы, большую роль играют взаимодействия между нуклонами.

Были исследованы свойства сверхплотной материи с различным набором частиц, такими как нейтроны, а также электроны и протоны. Также был исследован вклад различных частиц-переносчиков взаимодействия. Для достижения этих целей были рассмотрены различные потенциалы: потенциал Бета и Джонса, потенциал Skyrme, которые хорошо согласуются с экспериментальными данными. Кроме этого, вычисляется энергия системы, используя различные многочастичные методы: методы Хартри и Хартри-Фока, включая взаимодействие нуклонов. Благодаря этой информации рассчитываются термодинамические параметры, такие как давление, плотность энергии и скорость звука как функция плотности нейтронной звезды. Уравнения состояния вещества нейтронной звезды были сравнены между собой попарно, а затем были продемонстрированы тонкие отличия друг от друга.

Благодаря наблюдениям за миллисекундными пульсарами, которые являются одним из самых полезных астрофизических объектов для проверки фундаментальных законов физики были учтены последние наблюдательные ограничения на уравнение состояния. Показано, что наблюдательные данные требуют, чтобы уравнения состояния были жесткими, несмотря на то, что все жесткие уравнения состояния, в отличие от мягких, нарушают принцип причинности при больших плотностях. Наблюдательные ограничения были получены путем длительных наблюдений за пульсарами. При наблюдении за вращающимися пульсарами было обнаружено, что можно измерить физические параметры, которые позволяют вычислять массу самих пульсаров с помощью эффекта Шапиро. Путем объединения набора данных Североамериканской наногерцовой обсерватории гравитационных волн (NANOGrav) за 12,5 лет с недавними наблюдениями за орбитальной фазой, используя телескоп GreenBank, была измерена масса источника PSR J0740+6620 (нейтронная звезда), которая равна  $2,14_{-0,09}^{+0,10}$  солнечных масс. В качестве типичного наблюдательного ограничения на вращение нейтронных звезд, используются параметры источника PSR J1748-2246, считающегося вторым по скорости вращения пульсаром, а первым в настоящий момент считается XTEJ1739-285, совершающий 1122 оборота в секунду, хотя другие астрономы этого не подтвердили.

В заключение показано, что результаты вычисления без взаимодействия сильно разнятся с результатами уравнения состояния Бета и Джонса, где учитывался, как минимум, один переносчик взаимодействия. Также было определено, что зависимость полного радиуса звезды от центральной плотности, построенной на эмпирических соображениях, сильно отличается от результатов, полученных из уравнения состояния вырожденных нейтронных газов, начиная со значений плотности порядка ядерной. Новизна статьи заключается в исследовании нейтронных звезд путем сравнения современных наблюдательных данных и результатов, полученных с помощью применения различных уравнений состояния и на основе этого проведен анализ того какие из этих данных более подробно описывают физическую реальность.

**Ключевые слова:** уравнение состояния, нейтронная звезда, отношение масса-радиус, ядерные взаимодействия, наблюдательные ограничения.

#### Information about authors:

Tlemissov A., Al-Farabi Kazakh National University, Almaty 050040, Kazakhstan, master student, <https://orcid.org/0000-0003-3453-3465>, [Tlemissov-Ozzy@mail.ru](mailto:Tlemissov-Ozzy@mail.ru);

Tlemissova Zh., Al-Farabi Kazakh National University, National Nanotechnology Laboratory of Open Type Almaty 050040, Kazakhstan, lecturer, ORCID ID <https://orcid.org/0000-0003-0830-858X>, [kalymova160793@gmail.com](mailto:kalymova160793@gmail.com);

Boshkayev K., Al-Farabi Kazakh National University, Almaty 050040, Kazakhstan, associate professor, <http://orcid.org/0000-0002-1385-270X>, [kuntay@mail.ru](mailto:kuntay@mail.ru);

Urazalina A., Al-Farabi Kazakh National University, Almaty 050040, Kazakhstan, assistant professor, <https://orcid.org/0000-0002-4633-9558>, [y.a.a.707@mail.ru](mailto:y.a.a.707@mail.ru);

Quevedo H., Instituto de Ciencias Nucleares, Universidad Nacional Autonoma de Mexico, AP 70543, Mexico City 04510, Mexico, full professor, <http://orcid.org/0000-0003-4433-5550>, [quevedo@nucleares.unam.mx](mailto:quevedo@nucleares.unam.mx)

#### REFERENCES

- [1] S.L. Shapiro and S.A. Teukolsky. Black holes, white dwarfs, and neutron stars: the physics of compact objects (John Wiley & Sons, New York, 1983).
- [2] J.M. Lattimer and M. Prakash. The Physics of Neutron Stars. Science, 2004, Vol. 304, No 5670, P. 536–542.

- [3] I. Sagert, M. Hempel, C. Greiner, and J. Schaffner-Bielich. Compact stars for undergraduates, *European Journal of Physics*, 2006, Vol. 27, No 3, P. 577–610.
- [4] M. Rotondo, J.A. Rueda, R. Ruffini, and S. Xue, The self-consistent general relativistic solution for a system of degenerate neutrons, protons and electrons in  $\beta$ -equilibrium, *Physics Letters B*, 2011 Vol. 701, No 5, P. 667–671.
- [5] R.R. Silbar and S. Reddy, Neutron stars for undergraduates. *American Journal of Physics*, 2004, Vol. 72, No 7, P. 892–905.
- [6] I.S. Suh and G.J. Mathews, Cold Ideal EoS for Strongly Magnetized Neutron Star Matter: Effects on Muon Production and Pion Condensation, *Astrophys. J.*, 2001, Vol. 546, No 2, P. 1126–1136.
- [7] A. Potekhin, Physics of neutron star surface layers and their thermal radiation, I.Y.Yuan, X. Li, and D. Lai editors, *Astrophysics of Compact Objects*, American Institute of Physics Conference Series, 2008, Vol. 968 P. 121–128.
- [8] G. Baym, S. Furusawa, T. Hatsuda, T. Kojo, and H. Togashi, New Neutron Star EoS with Quark-Hadron Crossover, *Astrophys. J.*, 2019, Vol. 885, No 1, P. 42.
- [9] M. Rotondo, J. A. Rueda, R. Ruffini, and S. S. Xue, On the equilibrium of self-gravitating neutrons, protons and electrons in  $\beta$ -equilibrium, 2011, arXiv: 1107.2777.
- [10] H. T. Cromartie, E. Fonseca, S. M. Ransom, P. B. Demorest, Z. Arzoumanian, H. Blumer, P. R. Brook, M. E. De Cesar, T. Dolch, J. A. Ellis, R. D. Ferdman, E. C. Ferrara, N. Garver-Daniels, P. A. Gentile, M. L. Jones, M. T. Lam, D. R. Lorimer, R. S. Lynch, M. A. McLaughlin, C. Ng, D. J. Nice, T. T. Pennucci, I. H. Stairs, K. Stovall, J. K. Swiggum, and W. W. Zhu, Relativistic Shapiro delay measurements of an extremely massive millisecond pulsar, *Nature Astronomy*, 2020, Vol.4, P. 72–76.
- [11] B. Fuhrmeister and J. H. M. M. Schmitt, A systematic study of X-ray variability in the ROSAT all-sky survey. *Astron. Astrophys*, 2003, Vol. 403, P. 247–260.
- [12] F. M. Walter, T. Eisenbeiß, J. M. Lattimer, B. Kim, V. Hambaryan, and R. Neuhauser. Revisiting the Parallax of the Isolated Neutron Star RX J185635-3754 Using HST/ACS Imaging. *Astrophys. J.*, 2010, Vol. 724, No 1, P. 669–677.
- [13] K. Boshkayev, J. Rueda, and M. Muccino, Main parameters of neutron stars from quasi-periodic oscillations in low mass X-ray binaries. In M. Bianchi, R. Jantzen, and R. Ruffini, editors, 14th Marcel Grossmann Meeting - MG14, 2018, P. 3433–3440.
- [14] J.W.T. Hessels, S.M. Ransom, I.H. Stairs, P.C.C. Freire, V.M. Kaspi and F. Camilo. A Radio Pulsar Spinning at 716 Hz. *Science*, 2006, Vol. 311, No 5769, P. 1901–1904.
- [15] K. Boshkayev, N. Takibayev. Neutron stars: Physics (Properties and Dynamics, Nova Publishers 2017, P. 278).
- [16] R. Belvedere, K. Boshkayev, J. A. Rueda, and R. Ruffini, Uniformly rotating neutron stars in the global and local charge neutrality cases, *Nucl. Phys. A*, 2014, Vol. 921, P. 33–59.
- [17] Sh.R.Myrzakul, T.R.Myrzakul, F.B.Belisarova, Kh. Abdullayev, K.R. Myrzakulov. Noether symmetry approach in f-essence cosmology with scalar-fermion interaction. *News of the National Academy of Sciences of the Republic of Kazakhstan, Physico-Mathematical Series ISSN 1991-346X*, 2017, Vol. 5, No. 315, P. 163–171.
- [18] H. T. Cromartie, E. Fonseca, S. M. Ransom, P. B. Demorest, Z. Arzoumanian, H. Blumer, P. R. Brook, M. E. DeCesar, T. Dolch, J. A. Ellis, R. D. Ferdman, E. C. Ferrara, N. Garver-Daniels, P. A. Gentile, M. L. Jones, M. T. Lam, D. R. Lorimer, R. S. Lynch, M. A. McLaughlin, C. Ng, D. J. Nice, T. T. Pennucci, R. Spiewak, I. H. Stairs, K. Stovall, J. K. Swiggum, and W. W. Zhu. Relativistic Shapiro delay measurements of an extremely massive millisecond pulsar. *Nature Astronomy*, 2019, P. 439.
- [19] T. Yazdizadeh and G. H. Bordbar. The structure of cold neutron star with a quark core within the MIT and NJL models, 2019, arXiv:1906.00175.